



HAL
open science

Threshold of parametric decay instability accompagnying electron Bernstein wave heating in spherical tokamaks

Evgeniy Gusakov, Alexander Surkov

► **To cite this version:**

Evgeniy Gusakov, Alexander Surkov. Threshold of parametric decay instability accompagnying electron Bernstein wave heating in spherical tokamaks. 2004. hal-00001866v1

HAL Id: hal-00001866

<https://hal.science/hal-00001866v1>

Preprint submitted on 21 Oct 2004 (v1), last revised 16 Apr 2005 (v3)

HAL is a multi-disciplinary open access archive for the deposit and dissemination of scientific research documents, whether they are published or not. The documents may come from teaching and research institutions in France or abroad, or from public or private research centers.

L'archive ouverte pluridisciplinaire **HAL**, est destinée au dépôt et à la diffusion de documents scientifiques de niveau recherche, publiés ou non, émanant des établissements d'enseignement et de recherche français ou étrangers, des laboratoires publics ou privés.

Threshold of parametric decay instability accompanying electron Bernstein wave heating in spherical tokamaks

E Z Gusakov and A V Surkov

Ioffe Institute, Politekhnicheskaya 26, 194021 St. Petersburg, Russia

E-mail: a.surkov@mail.ioffe.ru

Abstract. The parametric instability of upper hybrid wave decay into back scattered upper hybrid wave and lower hybrid wave is considered for conditions of inhomogeneous plasma of spherical tokamaks. The possibility of absolute instability is demonstrated and the corresponding threshold is determined. It is shown that the threshold power increases with pump frequency and electron temperature. Threshold power is estimated for typical parameters of experiment in MAST tokamak. It is shown that in this case parametrical reflection arises, if probing power exceeds 129 W/cm^2 , which gives 40 kW for a beam of 10 cm radius.

1. Introduction

In recent years, considerable attention of the controlled fusion community has been paid to spherical tokamaks (ST). These are small aspect ratio devices with typically high plasma density and comparatively low magnetic field. This ST feature has strong effect on the electromagnetic wave propagation. In the microwave frequency region, characteristic surfaces, like the upper hybrid resonance and the cut-off are very close to the plasma edge. As a result, the electromagnetic (EM) waves are unable to penetrate into the plasma interior. The only way to overcome this difficulty is to use the linear conversion of the incident EM wave into the electron Bernstein wave (EBW) occurring in the upper hybrid resonance (UHR). The latter has no density limitations and can, in principle, carry the radio frequency power deep into the plasma. This mechanism of wave conversion has been successfully demonstrated to produce heating in over dense plasmas in the W7-AS stellarator [3]. The plasma heating experiment based on this scheme is in progress now in the MAST tokamak at Culham, UK. The wave propagation, conversion in the UHR and absorption is usually accompanied, in 100 kW power level experiments, by nonlinear effects, in particular, by parametric decay instabilities (Versator [1], FT-1 [2], W7-AS [3]). These instabilities lead to redistribution of incident power between plasma species and can cause anomalous reflection, especially when excited at the plasma edge.

The present paper is devoted to analysis of the decay instability thresholds and growth rates for specific conditions of low magnetic field typical for ST. The study is focused upon the decay of UH wave into another UH wave and intermediate frequency range wave satisfying the lower hybrid resonance condition, which was observed in the UHR heating experiments mentioned above. The influence of plasma inhomogeneity on its threshold is investigated for backscattering of the incident UH wave. Dependence of the decay instability threshold on the pump frequency, necessary for the heating experiment optimization, is studied.

The paper is organized as follows. In section 2 we deduce equations, describing the decay of the incident high-frequency UH wave into UH wave and low-frequency LH wave: $\ell_{UH} \rightarrow \ell'_{UH} + \ell_{LH}$, and consider them in WKB approximation. In section 3 we calculate an absolute instability threshold, which corresponds to UH wave induced back scattering instability. Brief discussion follows in section 4.

2. Equations for wave amplitudes

We use slab plasma model, i.e. density and magnetic field gradients are assumed to be along x axe. A magnetic field direction is chosen along z axe. We consider one dimensional problem of pump wave parametric decay. UH pump wave is supposed to be excited by external antenna via tunnelling effect ($X \rightarrow B$ scheme according to [4]), and assumed to propagate in x direction. We consider here the high pump frequency case, when the frequency is larger than doubled electron cyclotron frequency, corresponding to the magnetic field in UHR: $\omega_0 > 2\omega_{ce}$. In this case the UH pump wave dispersion curve (see figure 1) does not possess a turning point and transformation to Bernstein wave occurs without change of group velocity sign.

By indices $0, 1, 2$ we will mark frequency, wavenumber, complex amplitudes of the electric fields and potentials of the pump wave, parametrically reflected UH wave and LH wave correspondingly.

2.1. Nonlinear current and equation for LH wave

Poisson equation for LH waves can be represented in the following form [5]

$$\operatorname{div} \vec{D}_{LH} = \frac{d}{dx} \left[\left(\varepsilon(\omega_2) + \ell_T^2(\omega_2) \frac{d^2}{dx^2} \right) E_x^{LH} \right] + \eta(\omega_2) \frac{dE_z^{LH}}{dz} = 4\pi\rho_{LH} \quad (1)$$

Here $\vec{E}^{LH} = -\nabla\phi_{LH}$ is an electric field of LH wave, which is assumed to be potential, ε, η are the components of the dielectric tensor

$$\varepsilon(\omega) = 1 - \frac{\omega_{pe}^2}{\omega^2 - \omega_{ce}^2} - \frac{\omega_{pi}^2}{\omega^2 - \omega_{ci}^2}, \quad \eta(\omega) = 1 - \frac{\omega_{pe}^2}{\omega^2}$$

which for LH wave frequency $\omega_2 \sim \sqrt{\omega_{ce}\omega_{ci}}$ take the form

$$\varepsilon(\omega_2) \simeq 1 + \frac{\omega_{pe}^2}{\omega_{ce}^2} - \frac{\omega_{pi}^2}{\omega_2^2}, \quad \eta(\omega_2) \simeq -\frac{\omega_{pe}^2}{\omega_2^2}$$

Parameter ℓ_T is associated with particles thermal motion [6]

$$\ell_T^2(\omega) = \frac{3}{2} \left(\frac{\omega_{pe}^2}{\omega^2 - \omega_{ce}^2} \frac{V_{Te}^2}{\omega^2 - 4\omega_{ce}^2} + \frac{\omega_{pi}^2}{\omega^2 - \omega_{ci}^2} \frac{V_{Ti}^2}{\omega^2 - 4\omega_{ci}^2} \right) \quad (2)$$

where $V_{Te,i}$ corresponds to electron and ion thermal velocity $V_{Te,i} = (2T_{e,i}/m_{e,i})^{1/2}$. In particular, for LH wave (2) takes the form

$$\ell_T^2(\omega_2) \simeq \frac{3\omega_{pe}^2}{2\omega_{ce}^4} \left(\frac{1}{4}V_{Te}^2 + \frac{m_i}{m_e}V_{Ti}^2 \right)$$

Thus, equation (1), describing the excitation of LH wave, can be rewritten as

$$\text{div} \vec{D}_{LH} = -\ell_T^2(\omega_2)\phi_{LH}'''' - \varepsilon(\omega_2)\phi_{LH}'' - \varepsilon'(\omega_2)\phi_{LH}' + k_z^2\eta(\omega_2)\phi_{LH} = 4\pi\rho_{LH} \quad (3)$$

Here and below $'$ denotes d/dx . A charge density ρ is associated with nonlinear current j_{LH} by continuity equation

$$\frac{\partial\rho_{LH}}{\partial t} + \frac{\partial j_{LH}}{\partial x} = 0$$

To obtain nonlinear current j_{LH} we consider electron motion in the field of three potential waves

$$\begin{cases} \dot{v}_x = -\frac{e}{2m_e} \sum_{i=0,1,2} \left\{ E_i \exp \left[i \int^x k_i(x') dx' - i\omega_i t \right] + \text{c.c.} \right\} - \omega_{ce} v_y \\ \dot{v}_y = \omega_{ce} v_x \end{cases} \quad (4)$$

Here dot $\dot{}$ means d/dt . Electric field of three waves is taken in geometrical optics (or WKB) approximation. This approximation is not valid if the decay point x_d , determining in the inhomogeneous plasma by the conditions

$$k_0(x_d) = k_1(x_d) + k_2(x_d), \quad \omega_0 = \omega_1 + \omega_2 \quad (5)$$

is situated in the vicinity of LH wave turning point (see section 4 for proper discussion of corresponding criteria).

In deducing (1) we assumed following criteria to be satisfied

$$\frac{k_z^2 V_{Te}^2}{\omega_{ce}^2} \ll 1, \quad \frac{k_z^2 V_{Ti}^2}{\omega_2^2} \ll 1, \quad \left| \frac{\omega_2 - \omega_{ce}}{k_z V_{Te}} \right| \gg 1, \quad \left| \frac{\omega_2 - 2\omega_{ce}}{k_z V_{Te}} \right| \gg 1$$

First criterion, which characterizes $k\rho$ -approximation, allows us to get nonlinear component of a solution of (4) in the form

$$\begin{aligned} v_{LH} = \frac{e^2}{4m_e^2} \sum_{i,j=0,1,2} \frac{k_i}{\omega_j^2 - \omega_{ce}^2} \left\{ \frac{\omega_i + \omega_j}{(\omega_i + \omega_j)^2 - \omega_{ce}^2} E_i E_j \exp \left[i \int^x (k_i + k_j) dx' - i(\omega_i + \omega_j)t \right] \right. \\ \left. + \frac{\omega_i - \omega_j}{(\omega_i - \omega_j)^2 - \omega_{ce}^2} E_i E_j^* \exp \left[i \int^x (k_i - k_j) dx' - i(\omega_i - \omega_j)t \right] + \text{c.c.} \right\} \end{aligned}$$

Averaging v_{LH} we neglect high-frequency terms. That yields

$$\begin{aligned} \langle v_{LH} \rangle = \frac{e^2}{4m_e^2} \frac{\omega_1 - \omega_0}{(\omega_0 - \omega_s)^2 - \omega_{ce}^2} \left(\frac{k_0}{\omega_1^2 - \omega_{ce}^2} - \frac{k_1}{\omega_0^2 - \omega_{ce}^2} \right) E_0 E_1^* \\ \times \exp \left[i \int^x (k_0 - k_1) dx' - i(\omega_0 - \omega_1)t \right] + \text{c.c.} \end{aligned}$$

Taking into account that $j_{LH} = -en \langle v_{LH} \rangle$ and passing to the complex amplitudes of the potential $\phi_{LH} = (\phi_2 + \phi_2^*)/2$ one obtains an equation for LH wave

$$\begin{aligned} & -\ell_T^2(\omega_2)\phi_2'''' - \varepsilon(\omega_2)\phi_2'' - \varepsilon'(\omega_2)\phi_2' + k_z^2\eta(\omega_2)\phi_2 \\ &= \frac{e}{2m_e} \frac{\omega_{pe}^2}{\omega_{ce}^2} k_0 k_1 (k_0 - k_1) \left(\frac{k_0}{\omega_1^2 - \omega_{ce}^2} - \frac{k_1}{\omega_0^2 - \omega_{ce}^2} \right) \phi_0 \phi_1^* \\ & \quad \times \exp \left[i \int^x (k_0 - k_1) dx' - i(\omega_0 - \omega_1)t \right] \end{aligned} \quad (6)$$

2.2. Nonlinear current and equation for UH wave

For UH waves we have [5]

$$\begin{cases} \text{div} D_{UH} = \frac{d}{dx} \left[\left(\varepsilon(\omega_0) + \ell_T^2(\omega_0) \frac{d^2}{dx^2} \right) E_x^{UH} + ig(\omega_0) E_y^{UH} \right] = 4\pi\rho_{UH} \\ \frac{d^2}{dx^2} E_y^{UH} = ig(\omega_0) \frac{\omega_0^2}{c^2} E_x^{UH} \end{cases} \quad (7)$$

Here corresponding components of dielectric tensor take the following form for the frequency of UH wave $\omega_1^2 \approx \omega_{UH}^2 = \omega_{pe}^2 + \omega_{ce}^2$

$$\varepsilon(\omega_1) = 1 - \frac{\omega_{pe}^2}{\omega_1^2 - \omega_{ce}^2}, \quad g(\omega_1) \simeq \frac{\omega_{ce}}{\omega_1}$$

Parameter $\ell_T(\omega_1)$ can be represented as

$$\ell_T^2(\omega_1) = \frac{3V_{Te}^2}{2(\omega_1^2 - 4\omega_{ce}^2)} < \ell_T^2(\omega_2)$$

Considering potential UH wave $\vec{E}^{UH} = -\nabla\phi_{UH}$, and substituting integrated second equation of (7) to the first, one obtains

$$\text{div} \vec{\ell}_T^2(\omega_1)\phi_{UH}'''' - \varepsilon(\omega_1)\phi_{UH}'' - \varepsilon'(\omega_1)\phi_{UH}' + g^2(\omega_1) \frac{\omega_1^2}{c^2} \phi_{UH} = 4\pi\rho_{UH} \quad (8)$$

A charge density ρ_{UH} is associated with nonlinear current j_{UH} as

$$\frac{\partial \rho_{UH}}{\partial t} + \frac{\partial \langle j_{UH} \rangle}{\partial x} = 0, \quad j_{UH} = -e\delta n_{\omega_2} v_{\omega_0}$$

Here v_{ω_0} describes electron motion in the field of the pump wave

$$v_{\omega_0} = -\frac{1}{8\pi n e} \frac{\omega_{pe}^2 \omega_0}{\omega_0^2 - \omega_{ce}^2} \left\{ iE_0 \exp \left[i \int^x k_0(x') dx' - i\omega_0 t \right] + \text{c.c.} \right\}$$

Density modulation δn_{ω_2} is caused by the electron motion in the field of LH wave

$$\delta n_{\omega_2} = -\frac{1}{8\pi e} \frac{\omega_{pe}^2 k_2}{\omega_2^2 - \omega_{ce}^2} \left\{ iE_2 \exp \left[i \int^x k_2(x') dx' - i\omega_2 t \right] + \text{c.c.} \right\}$$

Here we omitted a contribution of LH wave component along the magnetic field, which is smaller in factor of $k_z^2 V_{Te}^2 / \omega_2^2 \ll 1$.

Averaging the nonlinear current, we leave the terms varying with frequency $\omega_0 - \omega_2$ only. That gives

$$\langle j_{UH} \rangle = \frac{1}{16\pi} \frac{e}{m_e} \frac{\omega_{pe}^2}{\omega_{ce}^2} \frac{\omega_0 k_2}{\omega_0^2 - \omega_{ce}^2} \left\{ E_0 E_2^* \exp \left[i \int^x (k_0 - k_2) dx' - i(\omega_0 - \omega_2)t \right] + \text{c.c.} \right\}$$

yielding (8) for the complex amplitude of the potential $\phi_{UH} = (\phi_1 + \phi_1^*)/2$ in the form

$$\begin{aligned} & -\ell_T^2(\omega_1)\phi_1'''' - \varepsilon(\omega_1)\phi_1'' - \varepsilon'(\omega_1)\phi_1' + g^2(\omega_1)\frac{\omega^2}{c^2}\phi_1 \\ & = \frac{e}{2m_e}\frac{\omega_{pe}^2}{\omega_{ce}^2}\frac{k_0k_2^2(k_0 - k_2)}{\omega_1^2 - \omega_{ce}^2}\phi_0\phi_2^* \exp\left[i\int^x(k_0 - k_2)dx' - i(\omega_0 - \omega_2)t\right] \end{aligned} \quad (9)$$

2.3. WKB-analysis of the equations obtained

A dispersion relations, which can be obtained from equations (3), (8), when $\rho_{UH} = \rho_{LH} = 0$, take the following form [5]: for UH waves

$$\varepsilon(\omega_{0,1}) = \ell_T^2(\omega_{0,1})\left(k_{0,1}^2 - \frac{k_*^4}{k_{0,1}^2}\right) \quad (10)$$

where the transformation wavenumber is

$$k_*^2 = \frac{\omega_0}{c}\frac{g}{\ell_T(\omega_0)} = \frac{\omega_{ce}/c}{\ell_T(\omega_0)}$$

and for LH waves

$$\varepsilon(\omega_2) = \ell_T^2(\omega_2)\left(k_2^2 + \frac{\varkappa_*^4}{k_2^2}\right), \quad \varkappa_*^4 = -\frac{\eta k_z^2}{\ell_T^2(\omega_2)} \quad (11)$$

Equations (10), (11) allow us to obtain group velocities of the corresponding waves. We get

$$v_{0,1} = \ell_T^2(\omega_{0,1})\frac{\omega_{0,1}^2 - \omega_{ce}^2}{\omega_{0,1}}\left(k_{0,1} + \frac{k_*^4}{k_{0,1}^3}\right), \quad v_2 = \ell_T^2(\omega_2)\frac{\omega_2\omega_{ce}^2}{\omega_{pe}^2}\left(k_2 - \frac{\varkappa_*^4}{k_2^3}\right) \quad (12)$$

One can see from (10),(11), (12) that in the probing frequency range under consideration $\omega_0 > 2\omega_{ce}$, which is used at present for EBW heating in MAST, there is no change of the group velocity sign in the UHR point. The transformation point of LH wave, which is shifted from LH resonance position (where $\varepsilon(\omega_2) = 0$), is the turning point of LH wave, and group velocity changes the sign there. Corresponding dispersion curves are represented in figure 1. We consider the most interesting case of $k_0 > 0$, $k_1 < 0$, when the group velocity directions give rise to positive feedback loop, which can lead to absolute decay instability [7, 8, 9, 10].

We consider equations (6), (9) in WKB approximation, substituting

$$\phi_{0,1,2} = \frac{a_{0,1,2}}{k_{0,1,2}\sqrt{v_{0,1,2}}}\exp\left[i\int^x k_{0,1,2}(x')dx' - i\omega_{0,1,2}t\right]$$

and neglecting corresponding small terms. In the vicinity of the decay point (5) we have

$$\begin{aligned} & \begin{cases} a_1^* = \nu_1 a_2 \exp\left[-i\int^x(k_0 - k_1 - k_2)dx'\right] \\ a_2' = \nu_2 a_1^* \exp\left[i\int^x(k_0 - k_1 - k_2)dx'\right] \end{cases} \\ & \nu_1 = -\frac{e}{4m_e}\frac{\omega_{pe}^2}{\omega_1\omega_{ce}^2}\frac{k_2 a_0^*}{\sqrt{-v_0 v_1 v_2}}, \quad \nu_2 = \frac{e}{4m_e}\frac{\omega_2}{\omega_0^2 - \omega_{ce}^2}\frac{k_2 a_0}{\sqrt{-v_0 v_1 v_2}} \end{aligned} \quad (13)$$

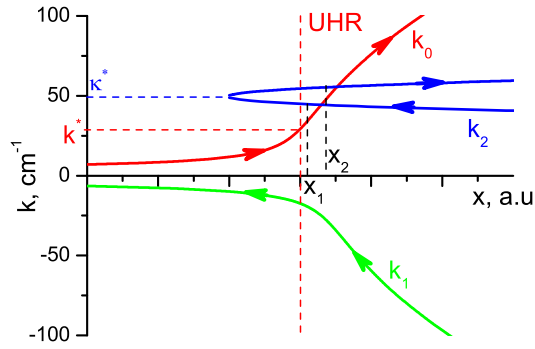


Figure 1. UH and LH waves dispersion curves in high frequency case ($\omega_0 > 2\omega_{ce}$).

3. Absolute instability threshold

Absolute instability can arise, when decay conditions (5) allow two decay points $x_{1,2}$ to exist, and the group velocities directions provide positive feedback loop. In this case, according to [9, 10], the absolute instability threshold is determined by the following conditions on the waves amplification coefficient

$$|S_{12}(x_1)| |S_{21}(x_2)| = 1 \quad (14)$$

where $S_{jk}(x_i)$ is the wave amplitude a_k , which leaves the vicinity of decay point x_i , due to incidence onto this point of the wave a_j of unit amplitude

$$S_{12} = -\frac{\nu_2 \ell \sqrt{-2\pi i}}{\Gamma(i|Z| + 1)} e^{\pi|Z|/2}, \quad S_{21} = \frac{\nu_1 \ell \sqrt{2\pi i}}{\Gamma(-i|Z| + 1)} e^{\pi|Z|/2}$$

where $Z = \ell^2 \nu_1 \nu_2$ and ℓ is the length of the decay region

$$\ell^2(x_d) = \left\{ \frac{d}{dx} [k_0(x) - k_1(x) - k_2(x)] \right\}^{-1} \Big|_{x=x_d}$$

The spectrum of the instabilities arising is determined by the condition on the phase, gained in the feedback loop

$$\Phi = \int_{x_1}^{x_2} [k_0(x') - k_1(x') - k_2(x')] dx' + \frac{\pi}{2} = 2\pi N, \quad N = 1, 2, \dots \quad (15)$$

To calculate the decay instability threshold we act in accordance with following procedure. We calculate the terms, involved in (14) using (15), and then substitute them to (14), obtaining an equation for threshold power.

At first we calculate the decay point coordinates $x_{1,2}$. It should be noted that the UHR position $x_{UH}(\omega_1)$ of the parametrically reflected UH wave is shifted in respect to the UHR position of the pump wave $x_{UH}(\omega_0)$. This shift can be estimated as

$$x_{UH}(\omega_1) - x_{UH}(\omega_0) = \frac{2L[x_{UH}(\omega_0)] \omega_0 \omega_2}{\omega_{pe}^2[x_{UH}(\omega_0)]}$$

$$L(x) = \left[\frac{1}{n} \frac{dn(x)}{dx} + \frac{2\omega_{ce}^2}{\omega_{pe}^2 B} \frac{dB(x)}{dx} \right]^{-1} \quad (16)$$

where $n(x)$, $B(x)$ are plasma density and magnetic field correspondingly. The decay points x_1 , x_2 are situated in the vicinity of pump wave UHR resonance $x_{UH}(\omega_0)$. It can be shown that for real plasma parameters the distance between UH resonances $x_{UH}(\omega_1) - x_{UH}(\omega_0)$ is substantial to provide

$$|k_1[x_{UH}(\omega_0)]| \sim \frac{\ell_T(\omega_0)k_*^2\omega_{pe}}{\sqrt{2\omega_0\omega_2}} \ll k_* = |k_0[x_{UH}(\omega_0)]|$$

This allows us to neglect $k_1(x_{1,2})$ in the decay condition (5), writing it as

$$k_0(x_{1,2}) = k_2(x_{1,2}) \quad (17)$$

To solve this equation we assume the dielectric permeability ε to vary linearly in the region considered

$$\varepsilon(x, \omega_0) = \frac{x - x_{UH}(\omega_0)}{L[x_{UH}(\omega_0)]}, \quad \varepsilon(x, \omega_2) = \frac{x - x_{LH}(\omega_2)}{L[x_{LH}(\omega_2)]}$$

and obtain from (10), (11), (17)

$$k_0^2(x_1) = k_2^2(x_1) = \frac{\tilde{\varkappa}_*^4}{\varkappa_{UH}^2}, \quad k_0^2(x_2) = k_2^2(x_2) = \varkappa_{UH}^2 \quad (18)$$

where following parameters are introduced

$$\tilde{\varkappa}_*^4 = \frac{\lambda_2^3 \varkappa_*^4 + \lambda_0^3 k_*^4}{\lambda_2^3 - \lambda_0^3} \simeq \varkappa_*^4, \quad \lambda_0^3 = L[x_{UH}(\omega_0)] \ell_T^2(\omega_0), \quad \lambda_2^3 = L[x_{LH}(\omega_2)] \ell_T^2(\omega_2)$$

and \varkappa_{UH} denotes the largest solution of the equation

$$\varkappa_{UH}^2 + \frac{\tilde{\varkappa}_*^4}{\varkappa_{UH}^2} = \frac{x_{UH}(\omega_0) - x_{LH}(\omega_2)}{\lambda_2^3 - \lambda_0^3}$$

Equations (18) determine in the indistinct form decay point positions in question. They allow us to calculate the parameters necessary for formulation of threshold power equation. In particular, the phase, gained in the feedback loop, can be represented as

$$\Phi = \frac{2}{3} \lambda_2^3 (k_2 - k_1)^3 + \frac{\pi}{2} \simeq \frac{2}{3} \lambda_2^3 \frac{(\varkappa_{UH}^2 - \varkappa_*^2)^3}{\varkappa_{UH}^3} + \frac{\pi}{2}$$

The length of the coherence region can be determined as

$$\ell^2(x_{1,2}) \approx \frac{2L(x_{1,2})\omega_0 v_0(x_{1,2})}{\omega_0^2 - \omega_{ce}^2} \quad (19)$$

Last important parameter is the value of LH wave group velocity in the decay points. It can be estimated as

$$-v_2(x_1) \simeq v_2(x_2) \simeq \ell_T^2(\omega_2) \frac{2\omega_2\omega_{ce}^2}{\lambda_2\omega_{pe}^2} \left[\frac{3}{2} \left(\Phi - \frac{\pi}{2} \right) \right]^{1/3}$$

We will be interested in the absolute instability threshold for mode $\Phi = 2\pi$. This mode has apparently almost the same threshold as fundamental mode $N = 0$, which has the lowest one, but still can be described in WKB approximation. In this case

$$|Z(x_1)| \simeq |Z(x_2)| \simeq -\ell(x_1)\ell(x_2)\nu_2(x_1)\nu_2(x_2)$$

and to estimate the threshold we should solve an equation

$$\frac{2\pi e^{\pi|Z|}}{|Z| |\Gamma(i|Z)|^2} = 1$$

which gives $|Z| \simeq 0.110$. Substituting obtained expressions for decay points (18) and coherence region length (19) to (13) one obtains, that $|Z|$ should be calculated as

$$|Z| = \frac{1}{2\sqrt{2}} \left(\frac{e}{4m_e} \right)^2 \frac{L^{4/3} \omega_{pe} \ell_T(\omega_0) k_*^2 \chi_*^2}{\omega_{ce}^4 \omega_0^{1/2} \omega_2^{3/2} \ell_T^{4/3}(\omega_2)} \left[\frac{3}{2} \left(\Phi - \frac{\pi}{2} \right) \right]^{-1/3} |a_0|^2$$

To obtain the threshold we take $|a_0|^2 = 8\pi P(\omega_0^2 - \omega_{ce}^2)/(\omega_0^2)$, where P is the pump wave power per unit square (in erg/(s · cm²)). Taking into account that for typical ST parameters in UHR $\omega_0 \sim \omega_{pe}$, and considering maximum $k_z \sim \omega_2/(3V_{Te})$, when we can neglect LH wave Landau damping, we obtain for $\Phi = 2\pi$ an equation for threshold power P^*

$$|Z| = 13.0 \left(\frac{e}{m_e} \right)^2 \frac{L^{4/3} \omega_{ce}^{1/6}}{c \omega_0^{5/6} V_{Te}^{10/3}} P^* = 0.110$$

which gives

$$P^* = 0.85 \cdot 10^{-2} c \left(\frac{m_e}{e} \right)^2 \frac{\omega_0^{5/6} V_{Te}^{10/3}}{L^{4/3} \omega_{ce}^{1/6}} \quad (20)$$

We calculate P^* for MAST tokamak parameters: $f_0 = \omega_0/(2\pi) = 57.5$ GHz, $T_e = 100$ eV, $B = 3.2$ kGs (in UHR position), $L = 5$ cm. In this case one obtains $P^* \simeq 1.29 \cdot 10^9$ erg/(s · cm²) = 1.29 MW/m², which gives for gaussian antenna beam with radius $\rho = 10$ cm threshold power $P_i^* \simeq 40$ kW.

4. Discussion

At first we discuss the approximations used. Our analysis is performed in WKB approximation, which holds true, when two following conditions are satisfied:

- Decay points $x_{1,2}$ are situated far enough from LH wave turning point x_* . More accurately, taking into account that electric field of LH wave in the vicinity of the turning point can be expressed in terms of Airy function, it can be written as

$$x_{1,2} - x_* \gg \ell_A \quad (21)$$

where Airy scale $\ell_A = 2^{2/3} \lambda_2$. In our case

$$\frac{x_{1,2} - x_*}{\ell_A} \simeq \left[\frac{3}{4} \left(\Phi - \frac{\pi}{2} \right) \right]^{2/3}$$

and the condition (21) can be shown to be satisfied even for $\Phi = 2\pi$.

- Length of decay region is not larger than Airy scale, which provides that all decay region is situated far enough from the turning point. The coherence region size (19) can be estimated as $\ell \simeq (2\lambda_0^3 \chi_*)^{1/2}$ and it can be shown that condition

$$\frac{\ell}{\ell_A} < 1 \quad (22)$$

can be satisfied for wide range ST experiment parameters.

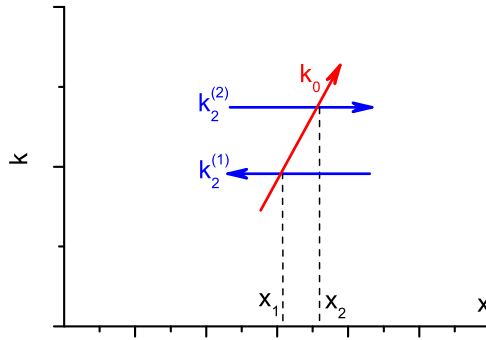


Figure 2. Approximate representation of the dispersion curves in the vicinity of decay points.

- The distance between extraordinary wave cut-off and UHR, which can be estimated as

$$\Delta x \simeq \frac{\omega_{ce}}{\omega_0} L$$

should be much larger than pump wavelength in the decay region. The last can be estimated as $\Lambda_0(x_{1,2}) \simeq 2\pi/\varkappa_*$. Corresponding condition, which provides WKB-representation of the UH waves to be correct, takes the form

$$\mu \equiv \frac{\omega_{ce}(x_{UH})L\varkappa_*}{2\pi\omega_0} \gg 1$$

This criterion is rather strict due to low magnetic field, which is typical for ST. But it can be shown to be satisfied for MAST experiment parameters, where $\mu \sim 6$.

Our consideration, which is based on the formulae (14), seems to be sensitive to the possibility to consider decay points as separate amplifiers of the incident wave. The condition for that is $x_2 - x_1 \gg \ell$, which is equivalent to

$$\frac{x_2 - x_1}{\ell} \simeq \left[\frac{3}{2} \left(\Phi - \frac{\pi}{2} \right) \right]^{1/3} \frac{\ell}{\lambda_2} \gg 1 \quad (23)$$

Comparing that with (22), one obtains that (23) can be satisfied for $\Phi = 2\pi$ in rather narrow range of parameters. But, actually, an accurate analysis shows, that for the dispersion curves behavior, which in the region in question can be approximated as in figure 2, the decay points joint influence is the same as given by our consideration.

Result obtained (20) gives the following scaling for threshold power

$$P^* [\text{W}/\text{cm}^2] = 1.6 \cdot 10^{-2} \left[\frac{\text{W} \cdot \text{T}^{1/6}}{\text{cm}^{2/3} \text{GHz}^{5/6} \text{eV}^{5/3}} \right] \cdot \frac{f_0^{5/6} T_e^{5/3}}{L^{4/3} B^{1/6}}$$

where $f_0[\text{GHz}]$ is the probing frequency, $T_e[\text{eV}]$ is the electron temperature, $L[\text{cm}]$ is the density inhomogeneity scale (16), $B[\text{T}]$ is the magnetic field in plasma.

5. Conclusion

In the paper absolute instability of parametrical reflection of upper hybrid wave is analyzed in WKB approximation. The reflection is assumed to be accompanied by radiation of lower hybrid wave. Equations, describing the decay, obtained in $k\rho$ -approximation. The decay threshold is determined. It is shown that threshold power increases with pump frequency and electron temperature. Threshold power is estimated for typical parameters of experiment in MAST tokamak. It is shown that in this case parametrical reflection arises, if probing power exceeds 129 W/cm^2 , which gives 40 kW in a beam of 10 cm radius.

Acknowledgments

The support of RFBR grants 04-02-16404, 02-02-81033 (Bel 2002-a) is acknowledged. A.V. Surkov is thankful to the “Dynasty” foundation for supporting his research.

References

- [1] McDermott F S, Bekefi G, Hackett K E, Levine J S and Porkolab M 1982 *Phys. Fluids* **25** 1488
- [2] Bulyginsky D G, Dyachenko V V, Irzak M A, Larionov M M, Levin L S, Serebrenniy G A and Shustova N V 1986 *Plasma Phys. Rep.* **2** 138
- [3] Laqua H P, Erckmann V, Hartfuß H J, Laqua H, W7-AS Team and ECRH Group 1997 *Phys. Rev. Lett.* **78** 3467
- [4] Ram A K, Bers A and Lashmore-Davies C N 2002 *Phys. Plasmas* **9** 409
- [5] Golant V E and Fedorov V I 1989 *RF Plasma Heating in Toroidal Fusion Devices* (New York, London: Consultants Bureau)
- [6] Akhiezer A I, Akhiezer I A, Polovin R V, Sitenko A G and Stepanov K N 1975 *Plasma Electrodynamics* (Oxford: Pergamon)
- [7] Rosenbluth M N 1972 *Phys. Rev. Lett.* **29** 564
- [8] White R, Lin C and Rosenbluth M N 1973 *Phys. Rev. Lett.* **31** 697, 1190
- [9] Piliya A D 1973 *Pis'ma v Zhurnal Eksperimental'noi i Teoreticheskoi Fiziki (JETP Letters)* **17** 374
- [10] Piliya A D and Fedorov V I 1974 *Zhurnal Tekhnicheskoi Fiziki (Sov. J. Tech. Phys.)* **43** 5